HHS Public Access

Author manuscript

MRS Adv. Author manuscript; available in PMC 2018 July 13.

Published in final edited form as:

MRS Adv. 2018 ; 3(30): 1677–1683. doi:10.1557/adv.2018.194.

Freeze-cast Porous Chitosan Conduit for Peripheral Nerve Repair

Kaiyang Yin[1], **Prajan Divakar**[1], **Jennifer Hong**[3], **Karen L. Moodie**[2,3], **Joseph M. Rosen**[1,2,3], **Cathryn A. Sundback**[4], **Michael K. Matthew**[2,3], and **Ulrike G.K. Wegst**[1]

[1]Thayer School of Engineering, Dartmouth College, Hanover, NH 03755, U.S.A

[2]Geisel School of Medicine, Dartmouth College, Hanover, NH 0375, U.S.A

[3]Dartmouth-Hitchcock Medical Center, Lebanon, NH 03756, U.S.A

[4]Center for Regenerative Medicine, Department of Surgery, Massachusetts General Hospital, Harvard Medical School, Boston, MA 02114, U.S.A

Abstract

A novel freeze-cast porous chitosan conduit for peripheral nerve repair with highly-aligned, double layered porosity, which provides the ideal mechanical and chemical properties was designed, manufactured, and assessed in vivo. Efficacies of the conduit and the control inverted nerve autograft were evaluated in bridging 10-mm Lewis rat sciatic nerve gap at 12 weeks post-implantation. Biocompatibility and regenerative efficacy of the porous chitosan conduit were evaluated through the histomorphometric analysis of longitudinal and transverse sections. The porous chitosan conduit was found to have promising regenerative characteristics, promoting the desired neovascularization, and axonal ingrowth and alignment through a combination of structural, mechanical and chemical cues.

INTRODUCTION

An estimated 2 million (5%) of the annual 40.2 million trauma-related emergency room admissions in the US require treatment for peripheral nerve injuries. These injuries occur in upper and lower extremities, and frequently result in permanent disabilities, such as numbness, weakness and pain. Although peripheral nerves possess the inherent ability to regenerate, nerve transections require surgical intervention to optimize functional recovery. While small gaps (≤5 mm) may be directly coapted, larger gaps (≥5 mm) require interposition grafting with nerve auto- or allografts or conduits to provide tension-free mechanical support, axon guidance, and protection from fibrous tissue ingrowth. Nerve guidance conduits (NGCs) avoid the substantial disadvantages of autografts such as a second surgical site, donor site morbidity, limited availability, and high treatment cost. However, peripheral nerve regeneration through NGCs has not yet matched that of autografts, the gold standard [1]. Efforts had been made to develop solid and rigid NGCs; they had the mechanical integrity to withhold suturing but with insufficient porosity to support nutrition and oxygen diffusion [2]. Porous scaffolds typically exhibit penetrating porosity; through tailoring the pore size, inflammatory infiltrate in the lumen can be minimized, while still allowing for sufficient nutrient transport [3].

Freeze casting generates porous materials with highly aligned porosity that can easily be tailored to best suit a given application, which is ideal for many structural and functional materials applications [4, 5]. Freeze casting is compatible with a broad range of water-soluble and water-dispersible biopolymers with minimal additives, making this a versatile and clean processing technique attractive for the fabrication of biomedical materials and devices [5, 6]. Chitosan, a biocompatible and biodegradable polysaccharide, has been evaluated and found to be a suitable material for a range of biomedical applications due to its superior mechanical properties and antimicrobial behaviour [7]. In particular, chitosan-based NGCs and tissue engineering scaffolds have been successfully manufactured for peripheral nerve regeneration [8, 9]. Our strategy is to fabricate, through a novel bi-directional freeze casting process, a porous chitosan conduit with two layers of radial pores and a non-porous membrane in between, which enhance the integrity and flexibility of the conduit, enable sufficient nutrition and oxygen flow, and minimize undesired cell infiltration by controlling the interlayer membrane thickness as well as the pore sizes.

MATERIALS AND METHODS

Materials

The following chemicals were used as received: chitosan powders (Chitosan 95/200, Heppe Medical Chitosan GmbH, Germany); 1-(3-Dimethylaminopropyl)-3-ethylcarbodiimide hydrochloride (A10807, Alfa Aesar, MA, USA); fluorescein sodium salt (F6377, Sigma-Aldrich, MO, USA).

Manufacture of the porous chitosan conduit

A 3.5 w/v% chitosan in 1.5 v/v% acetic acid solution was prepared on a roller mixer (W348923-A, Wheaton, NJ, USA) at 10 rpm for 24 hours. The chitosan solution was injected into the void between a coaxially fixed 4.2 mm inner diameter aluminium tube and a 2.0 mm diameter brass rod, and frozen for 20 minutes in a −80°C freezer (Model 5705, VWR, PA, USA). The frozen chitosan tube was demolded and lyophilized at 0.008 mbar and −85°C (FreeZone 6 Plus, Labconco, MO, USA) for 24 hours. The positive charge on chitosan was neutralized by 6 hours immersion in 0.4 v/v% sodium hydroxide solution in 95% ethanol. Finally, the chitosan tube was washed, flash frozen and lyophilized.

Structural characterization

The transversely and longitudinally sectioned conduits were gold sputter coated (Hummer 6.2, Anatech, CA, USA), and imaged by scanning electron microscopy (Tescan Vega3, Brno-Kohoutovice, Czech Republic). The conduit was stained with 0.05 mg/mL fluorescein sodium salt and 6 mM EDC in deionized water for 6 hours, followed by an 18-hour wash in PBS. Finally, it was imaged excited with 488 nm laser using a laser scanning confocal microscope (A1R, Nikon, Tokyo, Japan).

Radial compression testing of hydrated conduits

The porous chitosan conduits (12 mm) were immersed in phosphate buffered saline (PBS) for 24 hours before mechanical testing. The fully hydrated conduit was placed between Teflon coated compression platens; 50μL PBS were added to keep the conduit fully hydrated

throughout the testing. Mechanical properties and compression hysteresis of the conduit were determined with a microtester (Model 5848, Instron, MA, USA) at a compression rate of 0.5%/s to the maximum load of 0.5 N. The time-lapse video was recorded by a CCD camera (Edge AM3715TB, Dino-Lite, Taipei, Taiwan).

Animal protocol for in vivo testing

All animal tests were reviewed and approved by the Institutional Animal Care and Use Committee (IACUC) at Dartmouth College. The *in vivo* tests were performed with four female Lewis rats (180–240 g, Charles River, MA, USA). All animals (n = 2 for conduits and autografts, respectively) were anesthetized with isoflurane (3–5%) in oxygen. Ketoprofen and Lidocaine were given; the area around the incision site was shaved and disinfected with Betadine. General anaesthesia for the surgical procedure was maintained with 1.5–2% Isoflurane via nosecone. The animals were covered with sterile drapes around the surgical site. A 3 cm incision was made parallel to the femur. Blunt dissection through the vastus lateralis and biceps femoris muscle plains was performed to reveal the sciatic nerve. The sciatic nerve was dissected, and cut just above its trifurcation. Prior to implantation, the 12 mm long porous chitosan conduits were sterilized with ethylene oxide for 12 h before evacuation for 12 h. A 10 mm nerve gap was created and repaired either a with porous chitosan conduit or an autograft (a reversed nerve segment of the 10 mm as control) utilizing a surgical microscope; the nerve ends were sutured into the conduit using 9-0 nylon sutures. Finally, the skin incision was sutured closed. Two rats were kept in one cage under a 12 h day/night cycle and had free access to food and water before and after the surgery. Animals were sacrificed at 12 weeks and the chitosan-scaffold and autograft repaired nerves were harvested.

Histology

The harvested tissue was fixed in formalin. Proximal and distal nerve ends were longitudinally cut; the middle conduit was transversely cut. All samples were embedded in paraffin. The blocks were sectioned 4 μm thick. Slides were stained with H&E staining. Antigen retrieval was performed on sections for immunohistochemical (IHC) analysis using (Bond Epitope Retrieval 2, Leica, Germany) for 20 min at 100°C. The slides were blocked (Rodent Block R, RBR962G, Biocare, CA, USA) and incubated with anti-160 kD Neurofilament Medium (NF-9, 1:800, Abcam, MA, USA). Primary antibody binding was visualized using Bond Refine Detection kit (#DS9800, Leica, Germany) with DAB chromogen and hematoxylin counterstain. H&E and IHC stained slides were imaged with an upright Olympus BX50 microscope (Olympus, Japan).

DISCUSSION

Materials characterization

Two layers of highly-aligned, anisotropic, multi-domain porosity were observed by SEM (Figure 1A–D). The formation of two distinct structural layers agreed with the alignment of two opposite thermal gradients during freezing, due to the comparative thermal conductivity of brass and aluminium. No clear interface was observed between domains in a single layer; gradual transition of pore direction between the layers was observed instead. A thin

membrane had formed, designed to block cell infiltration and allow nutrition flow between the two layers. Fully hydrated conduits imaged by LSCM imaging revealed similar features, indicating open porosity both before and after implantation.

The compression testing and observed mechanical hysteresis of the porous chitosan conduit showed a fully recoverable behaviour (Figure 2) when fully hydrated. The virgin cycle deviated from the other cycles due to PBS redistribution and non-recoverable deformation (Figure 2B&D). The conduit first ovalized and offered low stiffness, then the wall of the conduit was compressed and showed increasingly higher stiffness due to compaction which results in an increased effective density; also the radially aligned porosity in the wall contributes to this effect. The membrane between the two layers further enhanced the resilience and integrity of the porous structure and assists the conduit to fully recover upon unloading.

IN VIVO TESTING IN RATS

The rats under study showed significant improvements in mobility during the twelve-week long recovery period after surgery. Resection of the sciatic nerve and freeze-cast porous chitosan conduit after sacrifice revealed no signs of abnormal nerve growth outside the conduit. A thin layer of encapsulation was visible around the conduit. Upon severing the distal portion of the nerve, a noticeable muscle twitch was observed, indicative of signal transduction.

Histopathological assessment both through H&E and IHC staining were consistent with gross observations (Figure 3A–F); a thin fibrous encapsulation dominated by fibroblasts (Figures 3A & 3G) was visible around the conduit in addition to extensive scaffold infiltration and collagen deposition (Figures 3B & 3G). Degradative macrophages and foreign body giant cells were observed in the pores of the conduit (Figure 3G). Also noteworthy was the angiogenesis in the lumen of the conduit; in particular, both the cellular connective structure around the nerve and the nerve itself were well vascularized (Figures 3B & 3C). NF-staining (Figures 3D–F & 3H) revealed regenerating peripheral nerve longitudinally oriented in the proximal, middle, and distal sections of the conduit. The nerve was noticeably smaller in its transverse diameter in the middle section, when compared to that of the proximal section, suggestive of an ongoing healing process.

CONCLUSION

The freeze-cast porous chitosan conduit demonstrated a microstructure and mechanical properties, in terms of its flexibility and full recovery after load relief, for successful surgical handling and implantation. The porous chitosan conduit successfully protected and promoted sciatic nerve regeneration in rats. After bridging 10 mm sciatic nerve defects in rats for 12 weeks, the axonal outgrowth through the conduit was observed with promising healing in terms of foreign body response and vascularization. In summary, freeze-cast porous chitosan conduits are very promising for application in peripheral nerve regeneration because they have the desired mechanical properties, both for handling by the surgeon and as tissue scaffold, and because they have a microstructure that prevents scar formation

within, which would obstruct it, while successfully promoting tissue regeneration and functional recovery.

Acknowledgments

The work was supported by a Synergy Translational Pilot Grant of Dartmouth College. The authors would like to thank the following people at Dartmouth College: Margaret S. Meacham (Center of Comparative Medicine and Research) for help with animal procedures, Scott M. Palisoul, David E. Beck and Rebecca R. O'Meara (Pathology Share Resource) for histological staining, Dr. Charles P. Daghlian (Electronic Microscope Facility) and Anne M. Lavanway (Class of 1978 Life Sciences Center) for their help with materials characterization.

References

1. Kehoe S, Zhang XF, Boyd D. Injury. 2012; 43(5):553–572. [PubMed: 21269624]
2. Gu X, Ding F, Yang Y, Liu J. Progress in Neurobiology. 2011; 93(2):204–230. [PubMed: 21130136]
3. Cerri F, Salvatore L, Memon D, Boneschi FM, Madaghiele M, Brambilla P, Del Carro U, Taveggia C, Riva N, Trimarco A, Lopez ID, Comi G, Pluchino S, Martino G, Sannino A, Quattrini A. Biomaterials. 2014; 35(13):4035–4045. [PubMed: 24559639]
4. Wegst UGK, Bai H, Saiz E, Tomsia AP, Ritchie RO. Nat Mater. 2015; 14(1):23–36. [PubMed: 25344782]
5. Hunger PM, Donius AE, Wegst UGK. Acta Biomaterialia. 2013; 9(5):6338–6348. [PubMed: 23321303]
6. Wegst UGK, Schecter M, Donius AE, Hunger PM. Philos Transact A Math Phys Eng Sci. 2010; 368(1917):2099–2121.
7. Croisier F, Jérôme C. European Polymer Journal. 2013; 49(4):780–792.
8. Riblett BW, Francis NL, Wheatley MA, Wegst UGK. Adv Funct Mater. 2012; 22(23):4920–4923.
9. Haastert-Talini K, Geuna S, Dahlin LB, Meyer C, Stenberg L, Freier T, Heimann C, Barwig C, Pinto LFV, Raimondo S, Gambarotta G, Samy SR, Sousa N, Salgado AJ, Ratzka A, Wrobel S, Grothe C. Biomaterials. 2013; 34(38):9886–9904. [PubMed: 24050875]

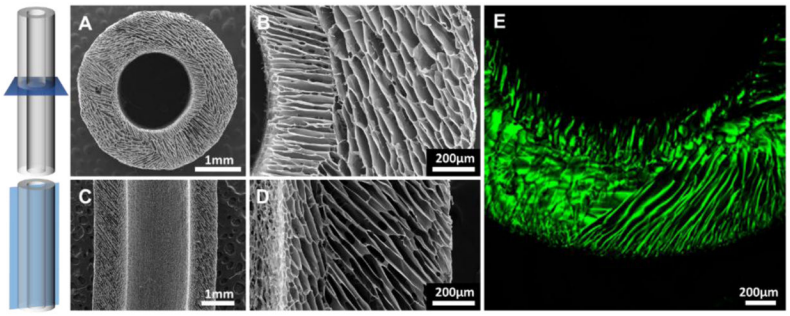

Figure 1.

SEM micrographs of (A, B) transverse and (C, D) longitudinal cross-sections of the conduit. (E) Confocal micrograph of the structure in the fully-hydrated state.

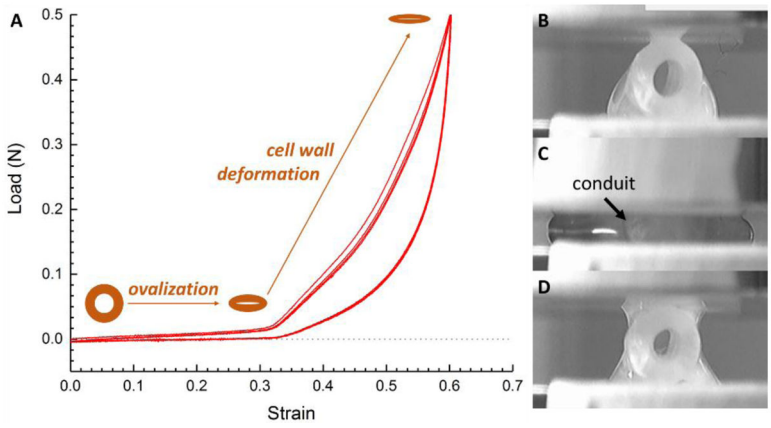

Figure 2.

Hysteresis of four radial compression-lease cycles (A) of the conduit, with optical micrographs of the conduit before (B) the first compression, at (C) maximum load, (D) and after unloading.

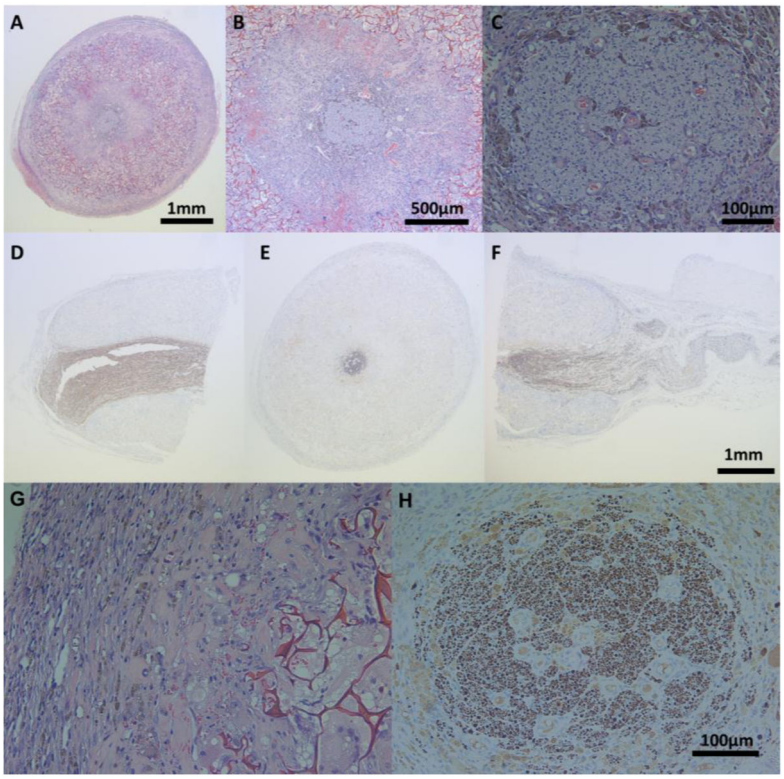

Figure 3.

H&E stained middle conduit sections in (A) 4X, (B) 10X, and (C) 40X and NF-9 stained (D) proximal, (E) middle, and (F) distal conduit sections of the regenerating sciatic nerve; 40X of H&E stained (G) middle section of the outer edge of the conduit, and NF-9 stained (H) middle sections of the regenerating sciatic nerve.